Organic & Biomolecular Chemistry

Cite this: *Org. Biomol. Chem.*, 2012, **10**, 2928

www.rsc.org/obc

COMMUNICATION

Relaxation of the rigid backbone of an oligoamide-foldamer-based α-helix mimetic: identification of potent Bcl-x_L inhibitors†

Jeremy L. Yap,[a] Xiaobo Cao,[b] Kenno Vanommeslaeghe,[a] Kwan-Young Jung,[a] Chander Peddaboina,[b] Paul T. Wilder,[c] Anjan Nan,[a] Alexander D. MacKerell, Jr,[a,d] W. Roy Smythe[b] and Steven Fletcher*[a,d]

Received 18th December 2011, Accepted 31st January 2012
DOI: 10.1039/c2ob07125h

By conducting a structure–activity relationship study of the backbone of a series of oligoamide-foldamer-based α-helix mimetics of the Bak BH3 helix, we have identified especially potent inhibitors of Bcl-x_L. The most potent compound has a K_i value of 94 nM *in vitro*, and single-digit micromolar IC_{50} values against the proliferation of several Bcl-x_L-overexpressing cancer cell lines.

The field of α-helix mimicry, in which small-molecule scaffolds are fashioned and appropriately functionalized to replicate the positioning of specific side chains on one face of an α-helix, has developed into a rational approach to disrupt protein–protein interactions in contemporary medicinal chemistry.[1–4] Pioneered largely by Hamilton,[5,6] α-helix mimicry has afforded inhibitors of several therapeutically significant protein–protein interactions that are mediated by α-helices, including Bak–Bcl-x_L[6,7] and p53–HDM2.[8] A variety of scaffolds has been designed, in particular the teraryls, the original of which is the 1,1′ : 4′,1″-terphenyl scaffold,[6] wherein the *ortho* positions are functionalized with appropriate side chains. This causes staggering of the rings through steric interactions, leading to effective mimicry of the *i*, *i* + 3/4 and *i* + 7 positions on one face of the α-helix. In addition, Hamilton introduced the oligoamide-foldamer approach to α-helix mimicry in which the integrity of the mimetic is maintained by the "folding" of the structure into an α-helical conformation through the assembly of a network of bifurcated hydrogen bonds.[9]

Over the last 10 years, many research groups have devised their own α-helix mimetic scaffolds that present key side chains in spatially similar loci to those adopted by the corresponding "parent" side chains on one face of the native α-helix.[10–15] Structure–activity relationship (SAR) studies of such α-helix mimetics focus on the variation of the appendages that project from the scaffold. However, an SAR analysis of the scaffold itself is lacking. In this manuscript, we investigate the significance of the backbone identity of a series of oligoamide-foldamer-based α-helix mimetics, as evaluated by molecular modeling and dynamics simulations, disruption of the Bak–Bcl-x_L complex *in vitro* and proliferation inhibition of Bcl-x_L-overexpressing cancer cells.

Proteins in the B-cell lymphoma (Bcl-2) family are critical regulators of programmed cell death, or apoptosis.[16] Bcl-x_L and Bcl-2 are two such family members that inhibit apoptosis; conversely, Bak and Bax are pro-apoptotic members. Bcl-x_L is overexpressed in many types of cancer,[17] including mesothelioma,[18] non-small cell lung[19] and colon cancers,[20] contributing to tumour initiation and progression as well as to resistance to chemo- and radiotherapies.[21,22] Bcl-x_L is able to inhibit Bak- and Bax-mediated apoptosis by sequestering the proteins through their B-cell homology 3 (BH3) "death" domains.[16] The Bak BH3 domain is α-helical, and, by NMR solution studies and alanine scanning, it has been demonstrated that four hydrophobic residues, Val74 (*i*), Leu78 (*i* + 4), Ile81 (*i* + 7) and Ile85 (*i* + 11), all of which lie on one face of the helix, are involved in binding.[23] The NMR solution structure of the Bak–Bcl-x_L complex (PDB ID: 1BXL) is shown in Fig. 1A, as is that of the Bak BH3 α-helix in Fig. 1B. Towards the development of novel, anti-cancer therapeutics, the disruption of the Bak–Bcl-x_L interaction by small-molecule mimicry of the Bak BH3 α-helix is an area of active research.[7,9,24–29] Hamilton has achieved low micromolar disruption of the Bak–Bcl-x_L complex *in vitro* with a synthetic α-helix mimetic (**1**; Fig. 1C) of the Bak BH3 domain based on an oligoamide-foldamer strategy.[9] Composed of three identical pyridine-based subunits, the structure projects three isopropyl groups such that their relative positions effectively mimic the side chains of Val74, Leu78 and Ile81.

A crystal structure of an analogue of **1** revealed that the pyridine nitrogen atoms are engaged in bifurcated hydrogen bonds,[9] rigidifying the backbone of the mimetic, whilst also inducing a

[a]*Department of Pharmaceutical Sciences, University of Maryland School of Pharmacy, 20 N Pine St, Baltimore, MD 21201, USA. E-mail: sfletche@rx.umaryland.edu; Fax: +1 410 706 5017; Tel: +1 410 706 6361*
[b]*Scott & White Memorial Hospital, 702 SW HK Dodgen Loop Room 219, Temple, TX 76504, USA*
[c]*Department of Biochemistry and Molecular Biology, University of Maryland School of Medicine, 108 N Greene St, Baltimore, MD 21201, USA*
[d]*University of Maryland Marlene and Stewart Greenebaum Cancer Center, 22 S Greene St, Baltimore, MD 21201, USA*

†Electronic supplementary information (ESI) available: All synthetic procedures, characterization data and ^1H and ^{13}C NMR spectra of intermediates **7–20f** and final compounds **1–6**; molecular dynamics simulation data; procedures for the *in vitro* fluorescence polarization assay and the XTT whole cell toxicity assay. See DOI: 10.1039/c2ob07125h

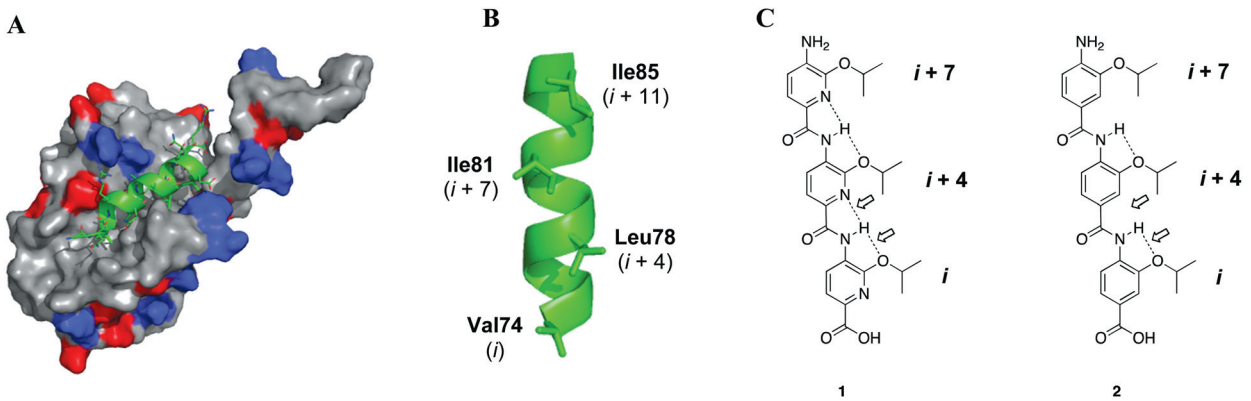

Fig. 1 A. PyMOL[34] representation of the NMR solution structure of the Bak–Bcl-x_L complex (PDB ID: 1BXL);[23] Bcl-x_L: uncharged amino acids in grey, acidic residues in red, basic residues in blue; Bak BH3 peptide in green (coloured by atom type). B. The Bak BH3 α-helix (PDB ID: 1BXL), illustrating the staggered arrangement of the key hydrophobic amino acids (highlighted as stick representations) and their location on the same face of the helix. C. The structures of the picolinamide α-helix mimetic **1** and its benzamide analogue **2**; dashed lines indicate hydrogen bonds; arrows indicate hydrogen bond lengths studied.

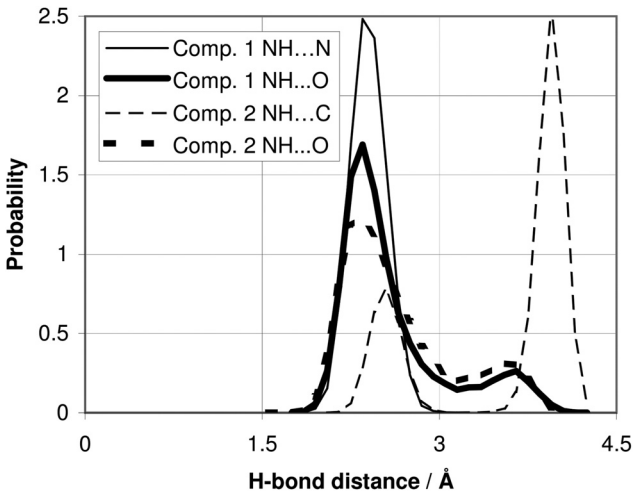

Fig. 2 Probability distribution for the C-terminal bifurcated hydrogen bond lengths in **1** and the analogous distances in **2**, indicated by the arrows in Fig. 1c.

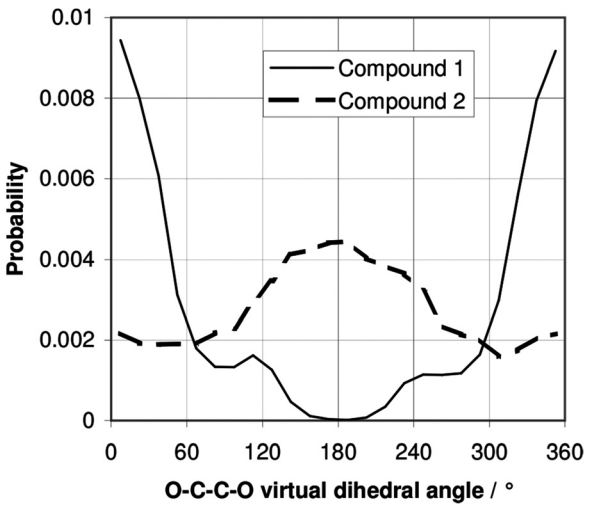

Fig. 3 Probability distribution for the C-terminal virtual dihedral angle defined by (1) the ether oxygen of residue *i*, (2) its *N*-substituted aromatic carbon, (3) the same *N*-substituted aromatic carbon of residue *i* + 4, and (4) the ether oxygen of residue *i* + 4 in compounds **1** (continuous curve) and **2** (broken curve).

degree of curvature.[30] However, it is not clear if such a constraining network of hydrogen bonds would be present under physiological conditions. To examine this possibility, 50 ns molecular dynamics (MD) simulations in explicit water were performed on picolinamide **1** and the benzamide analogue **2**[31] (Fig. 1C) – the latter of which is incapable of forming intramolecular bifurcated hydrogen bonds – using the program CHARMM[32] with the CHARMM General Force Field.[33] Computational details can be found in the ESI.† Fig. 2 shows the calculated probability distribution for the C-terminal bifurcated hydrogen bond lengths in **1** and **2** (indicated by the arrows in Fig. 1C); the thin, continuous line represents the hydrogen bond between the amide NH of the C-terminal subunit of **1** and the central pyridine N, whilst the thick, continuous line represents the hydrogen bond between the same amide NH and its ether O. Similarly, the thin, broken line represents the distance between the amide NH of **2** and the analogous C of the central benzene ring, while the thick, broken line represents the hydrogen bond between the same amide NH and its ether O. As is evident, the NH···N hydrogen bond is more stable than the NH···O interaction; on the time scale of our MD simulation, the former has no probability density above 3.1 Å, while the latter has a significant probability corresponding to non-hydrogen bonded conformations. The same plot for the N-terminal bifurcated hydrogen bond is nearly identical, and the plots for the NH···O distances in compound **2** are similar, except that they are slightly broadened, which is probably a result of the greater conformational flexibility associated with the loss of the amide NH to pyridine N hydrogen bond that is present in **1**.

We subsequently examined the solution-phase propensity of compounds **1** and **2** for presenting the isopropyl ether groups in the orientation required to mimic the *i*, *i* + 4 and *i* + 7 positions of the Bak BH3 α-helix. Specifically, the virtual dihedral angle defined by (1) the ether oxygen of residue *i*, (2) its *N*-substituted

Table 1 Measurements of selected distances and angles in Sattler *et al.*'s Bak–Bcl-x_L NMR structure[23] compared to corresponding average and median values from 50 ns MD simulations on compounds **1** and **2**

		Oligoamide-foldamer[a]		
Bak BH3 α-helix			**1**	**2**
$V74C^{\alpha}$–$L78C^{\alpha}$/Å	6.2	Average O1–O2/Å	6.1 ± 0.6	7.6 ± 1.0
$V74C^{\alpha}$–$L78C^{\beta}$/Å	5.7	Median O1–O2/Å	5.9	8.0
$L78C^{\alpha}$–$I81C^{\alpha}$/Å	5.8	Average O2–O3/Å	6.1 ± 0.7	7.7 ± 0.9
$L78C^{\beta}$–$I81C^{\alpha}$/Å	7.2	Median O2–O3/Å	5.9	8.1
$V74C^{\alpha}$–$I81C^{\alpha}$/Å	11.5	Average O1–O3/Å	11.8 ± 0.8	13.3 ± 0.7
		Median O1–O3/Å	11.8	13.4
$V74C^{\alpha}$–$L78C^{\alpha}$–$I81C^{\alpha}$/°	144	Average O1–O2–O3/°	156 ± 11	127 ± 21
$V74C^{\alpha}$–$L78C^{\beta}$–$I81C^{\alpha}$/°	124	Median O1–O2–O3/°	157	125

[a] O1, O2 and O3 respectively correspond to the C-terminal, middle and N-terminal ether oxygens in the oligoamide-foldamers. Averages are given ± the corresponding standard deviation.

aromatic carbon, (3) the same *N*-substituted aromatic carbon of residue $i + 4$, and (4) the ether oxygen of residue $i + 4$ was measured. Fig. 3 shows the probability distribution of the C-terminal instance of this virtual dihedral in compounds **1** and **2**. In the presence of the bifurcated hydrogen bond (Fig. 3: compound **1**, continuous curve), the conformation at 0° (*i.e.* with the ether oxygen atoms pointing in the same direction) is strongly favoured, and there is no sampling at 180°, although small shoulders can be observed around 120° and 240°. Conversely, without a bifurcated hydrogen bond (Fig. 3: compound **2**, broken curve), the dihedral between the two aromatic rings essentially acts as a free rotor, with a relatively weak preference towards 180°. Again, the same plot of the N-terminal virtual dihedral is nearly identical (ESI†).

Finally, the propensity for the ether oxygen atoms in compounds **1** and **2** to mimic the positions of the corresponding atoms in Sattler *et al.*'s NMR structure of the Bak peptide in complex with Bcl-x_L (PDB ID: 1BXL)[23] was studied by means of measuring the distances and angles between these atoms. Table 1 shows the average and median values for the O1–O2–O3 angle in the oligoamide-foldamers; the full probability distributions can be found in Fig. A in the ESI.† O1, O2 and O3 respectively correspond to the C-terminal, middle and N-terminal ether oxygens. The geometry of the O1–O2–O3 angle in compound **1** is in good agreement with the $V74C^{\alpha}$–$L78C^{\alpha}$–$I81C^{\alpha}$ angle in Bak. As a result of the increased conformational flexibility, the average and median distances are uniformly too large in compound **2**, and the angle is significantly smaller, bringing the O1–O2–O3 angle in **2** in closer agreement with the $V74C^{\alpha}$–$L78C^{\beta}$–$I81C^{\alpha}$ angle in Bak. These data demonstrate that both the rigid picolinamide **1** and the more flexible benzamide **2** are good mimetics of the orientation of the side chains being projected from the Bak BH3 α-helix in aqueous solution.

Whilst both **1** and **2** present their side chains in orientations that adequately mimic those adopted by Val74, Leu78 and Ile81 in the Bak–Bcl-x_L structure, in terms of relative affinities we postulated that oligoamides of reduced rigidities (*i.e.* of increased benzene-to-pyridine ratios) would afford Bcl-x_L inhibitors of greater potencies than the rigid oligoamide **1** for the following reasons. Fig. 1B shows the *staggered* arrangement of the side chains of the hydrophobic amino acids Val74, Leu78, Ile81 (and Ile85) that occur on one face of the Bak BH3 α-helix. The side chains of oligoamide **1**, as a direct consequence of intramolecular bifurcated hydrogen bonding, are *eclipsed* rather than staggered. It was anticipated that there would be a more favourable enthalpic term with oligoamides of greater flexibilities/reduced rigidities as they may more readily assume a (staggered) conformation that maximizes interactions with the binding surface, a phenomenon that may not be accessible to compounds whose conformations are "locked" by bifurcated hydrogen bonds. In addition, since the hydrophilic pyridine nitrogens may be poorly tolerated in the hydrophobic crevice, it was anticipated that the more hydrophobic the oligoamide, the more thermodynamically favourable would be its binding to Bcl-x_L.

Design and synthesis

In order to investigate the SAR of the oligoamide scaffold, we prepared the novel compounds **3**, **4**, **5** and **6**, along with the previously synthesized compounds **1**[9] and **2**;[31] their structures are

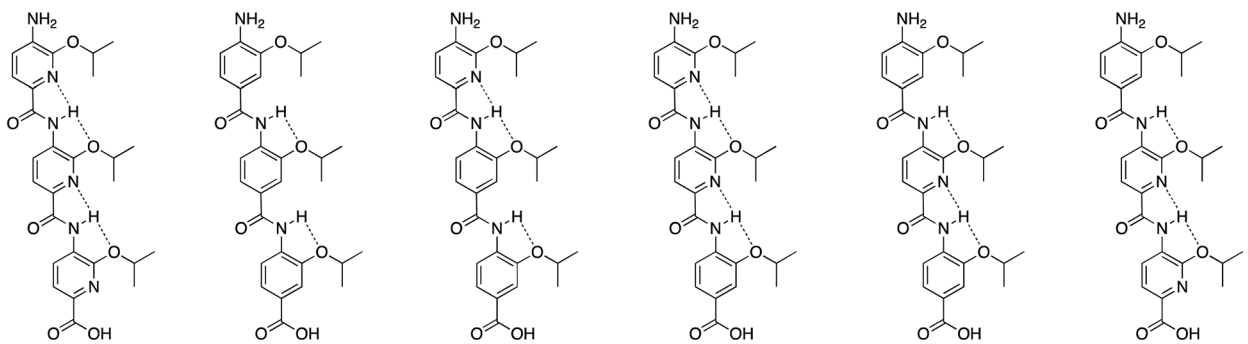

Fig. 4 Structures of the target molecules prepared in this study, along with their predicted log *P* values.[35] Dashed lines indicate hydrogen bonds.

given in Fig. 4. The distribution of pyridine *versus* benzene rings was selected to systematically control the extent of intramolecular hydrogen bonding in the proteomimetics, thereby controlling the extent of conformational flexibility. The predicted log *P* value of each compound, which is a measure of lipophilicity/hydrophobicity, is also given.[35] A simple retrosynthetic analysis of the target molecules **1–6** reveals they can be accessed from the conjugation of otherwise identical benzene and/or pyridine monomers. The requisite benzene monomers **7** and **8** were prepared as described previously (Scheme 1).[31] Briefly, esterification of the carboxylic acid of 3-hydroxy-4-nitrobenzoic acid (**9**) gave methyl ester **10**. Alkylation of the phenol with isopropyl alcohol under Mitsunobu conditions furnished compound **11** in excellent yield. Subsequently, saponification of the methyl ester gave acid **7** quantitatively, whilst reduction of the nitro group delivered aniline **8**. The original route to prepare the pyridine monomers **12** and **13** is lengthy[9] and proceeds *via* a pyridone functionality whose regioselective alkylation can be non-trivial.[36] Our alternative route (Scheme 2) is shorter, higher-yielding and by-passes the potentially-problematic pyridone stage. Furthermore, this chemistry works well with a wide range of other alcohols,[37] facilitating the development of future congeners of the desired subunits. The key step in our approach is the *ortho*-selective nucleophilic aromatic substitution (S_NAr) of 2,6-dichloropyridine (**14**) with sodium isopropoxide. We observed excellent *ortho*-regiochemical control in non-polar solvents, which we have ascribed to coordination of the sodium counterion (which remains associated with the isopropoxide anion in non-polar solvents) to the *ortho* nitro group as this would lead to a cyclic, 6-membered transition state.[37] A Stille coupling of **15** with (tri-n-butyl)vinyltin introduced a vinyl group *para* to the nitro function (compound **16**), which was then oxidatively cleaved with $KMnO_4$ to give acid **12**. Esterification and reduction as with the benzene subunit synthesis afforded the final monomer **13**.

All target compounds, including the previously-reported molecules **1** and **2**, were prepared through the assembly of either the benzene subunits **7** and **8** and/or pyridine subunits **12** and **13** as appropriate (Scheme 3). Couplings of carboxylic acids to anilines were accomplished through the *in situ*-generated acid chlorides with PPh_3Cl_2 to give the nitro dimers **17**, which were subsequently reduced to the corresponding anilines **18** in excellent overall yields of more than 80%. The sequence of coupling-reduction was repeated once more, followed by saponification of the methyl esters to give the final molecules **1–6** in quantitative yields.

Zhang *et al.* have previously described a fluorescence polarization (FP) competition assay using an FITC (fluorescein isothiocyanate)-N-terminus-labeled 16-mer Bak-BH3 peptide to determine the K_i values of inhibitors of the Bcl-x_L protein.[38] We conducted the assay as previously described, although a 6-aminohexanoic acid (Ahx) spacer was added in between the N-terminus of the Bak peptide and the FITC fluorophore so that the fluorescent peptide used was FITC-Ahx-GQVGRQLAIIGD-DINR-NH_2. Titration of the fluorescent peptide with Bcl-x_L revealed its binding affinity (K_d) to be 12.5 nM, which is in good agreement with the peptide lacking the Ahx linker.[38] Results for the present compounds **1–6** in the competition assay are reported in Table 2; K_i values were determined by entering

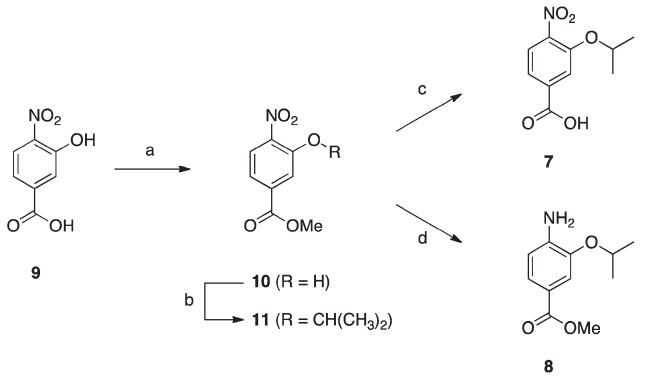

Scheme 1 (a) $SOCl_2$, MeOH, reflux, 12 h, 100%; (b) 1. isopropyl alcohol, PPh_3, THF, rt, 2 min; 2. DIAD, 16 h, 83%; (c) $LiOH{\cdot}H_2O$, THF–MeOH–H_2O, 3 : 1 : 1, rt, 1 h, 95%; (d) H_2, 10% Pd/C, MeOH, rt, 16 h, 95%.

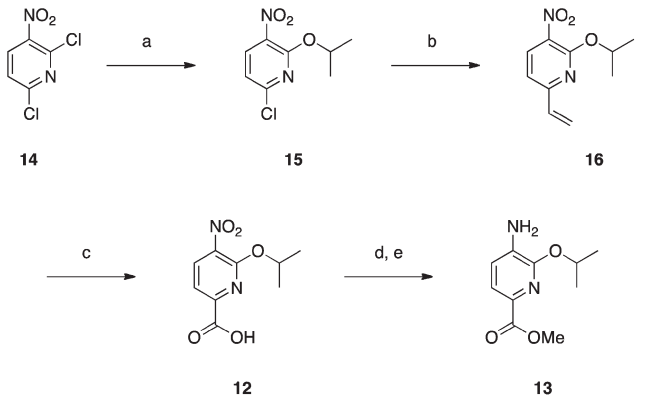

Scheme 2 (a) Isopropanol, NaH, toluene, 0 °C to rt, 16 h, 98%; (b) $(n\text{-}Bu)_3SnCH{=}CH_2$, $Pd(PPh_3)_4$, DMF, 120 °C, 16 h, 91%; (c) $KMnO_4$, acetone–H_2O, 1 : 1, rt, 12 h, 74%; (d) $SOCl_2$, MeOH, reflux, 12 h, 100%; (e) $SnCl_2{\cdot}2H_2O$, EtOAc, 50 °C, 12 h, 96%.

the appropriate IC_{50} value into the Cheng–Prusoff equation.[39] The principal trend is that the stepwise replacement of the pyridine subunits with benzene subunits led to an increase in Bcl-x_L inhibition, with the least potent compound picolinamide **1** (K_i = 970 nM) and the most potent compound benzamide **2** (K_i = 94 nM). Presumably, this is a consequence of the increased conformational flexibility of **2**, allowing it to better undergo more favourable interactions with the Bcl-x_L hydrophobic crevice, in combination with its increased hydrophobicity. More particularly, comparing the data for compounds **1** and **4**, whose structures exhibit identical bifurcated hydrogen bonding, reveals a three-fold improvement in Bcl-x_L inhibition that must be attributed to the greater hydrophobicity of **4**. Consistent with this are the relative affinities of **5** and **6**. Collectively, these data indicate that the ability of an oligoamide-foldamer to form bifurcated hydrogen bonds reduces its inhibitory activity against Bcl-x_L, and that the inclusion of hydrophilic nitrogen atoms on the hydrophobic face is not tolerated.

We also evaluated the effects of our compounds in cancer cells that harbour high expression levels of Bcl-x_L. Since the binding of our small-molecules to the hydrophobic BH3-binding domain of Bcl-x_L would disable its anti-apoptotic function, it is

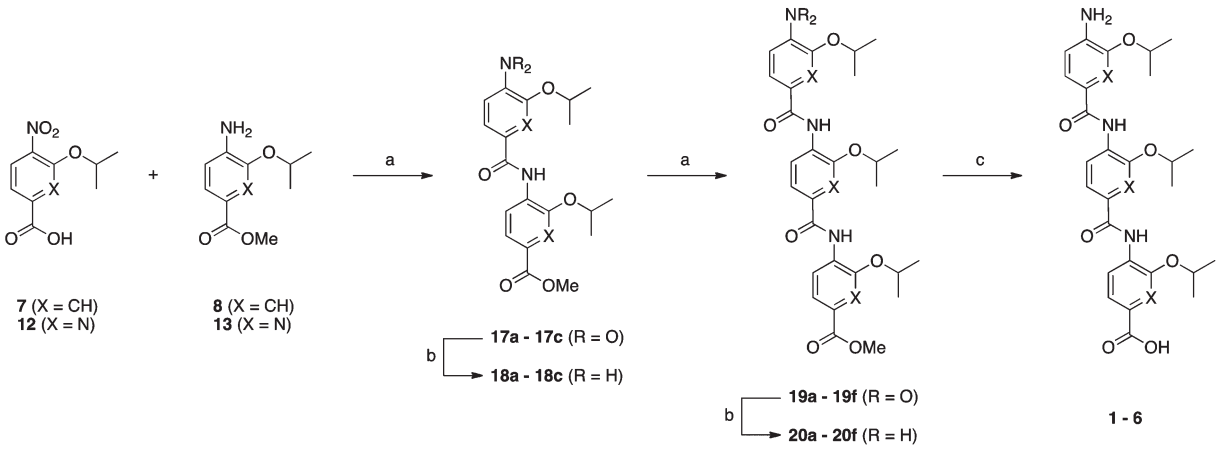

Scheme 3 (a) PPh_3Cl_2, $CHCl_3$, reflux, 2–12 h, 90–100%; (b) $SnCl_2{\cdot}2H_2O$, EtOAc, 50 °C, 12 h, 83–100%; (c) NaOH, THF–MeOH–H_2O, 3 : 1 : 1, rt, 95–100%.

Table 2 Thermodynamic parameters for the disruption of the Bak–Bcl-x_L interaction by α-helix mimetics **1–6**, as determined by an *in vitro* fluorescence polarization (FP) assay

	Fluorescence polarization (FP, nM)	
Compound	IC_{50}	K_i
1	2139 ± 387	970 ± 176 (2300[9])
2	207 ± 11	94.0 ± 5.0
3	297 ± 217	135 ± 98
4	738 ± 326	335 ± 148
5	394 ± 54	179 ± 24
6	584 ± 163	265 ± 74

Table 3 Cell proliferation inhibition of several Bcl-x_L-overexpressing cell lines by α-helix mimetics **1–6**, as determined by an XTT assay; ND = not determined

	Cell line (IC_{50}, μM)			
Compound	DLD-1	I45	H1299	A549
1	2.0 ± 0.1	4.3 ± 0.1	2.2 ± 0.1	1.1 ± 0.1
2	9.2 ± 0.8	4.1 ± 0.3	3.9 ± 0.7	4.4 ± 0.9
3	28 ± 2	22 ± 1	17 ± 2	ND
4	64 ± 10	53 ± 7	48 ± 5	ND
5	4.2 ± 0.1	5 ± 0.1	6.3 ± 0.7	11 ± 1
6	ND	ND	5.2 ± 0.8	ND

anticipated that these small-molecules would induce apoptosis in these cell lines. The cancer cell lines investigated were DLD-1 (colon cancer),[40] I45 (mesothelioma),[41] H1299 (non-small cell lung cancer)[19] and A549 (adenocarcinoma).[19] Briefly, cells were incubated with various concentrations of the compounds for 72 h, then cell viability was determined by conducting an XTT assay (ESI†). The data in Table 3 clearly demonstrate that most oligoamides were potent inhibitors of the proliferation of Bcl-x_L-overexpressing cell lines, particularly compounds **1**, **2** and **5**, with minimal toxicity towards untransformed human lung microvascular endothelial cells (HMVEC; **1**: IC_{50} = 19 μM, **2**: IC_{50} = 28 μM, **5**: IC_{50} = 36 μM). However, the whole cell data do not mirror the *in vitro* FP data. In particular, oligoamide **1**, which was the least potent *in vitro*, was consistently the most cytotoxic. This may be a consequence of differences in cell uptake. Moreover, since our inhibitors are rather simple molecules whose activities are presumably dominated by hydrophobic–hydrophobic interactions, it is likely that these compounds suffer from a variety of off-target effects, which may further explain the disparity between the *in vitro* and whole cell evaluations. For example, analogous to Bcl-x_L, the related Bcl-2 proteins Bcl-2 (*e.g.* PDB ID: 2XA0) and Mcl-1 (*e.g.* PDB ID: 3PK1),[23] as well as the non-Bcl-2 family member HDM2 (*e.g.* PDB ID: 1YCR),[42] all possess a hydrophobic crevice that recognizes the hydrophobic face of its α-helix protein partner. To investigate this further, we transfected Bak siRNAs into A549 cells, and evaluated the cytotoxic effects of compounds **1**, **2** and **5**. At 20 μM inhibitor, compound **1** was twice as cytotoxic as **2** and **5**. Since the pro-apoptotic protein Bak had been silenced, these findings suggest that the increased cytotoxicity of **1** was due to the antagonism of biological targets other than the Bak–Bcl-x_L complex. Furthermore, at lower doses, analogous experiments with Bcl-x_L siRNAs led to increased cytotoxic sensitivities to the oligoamides **1**, **2** and **5**, relative to cells treated with control siRNAs, indicating that these compounds have anti-apoptotic protein targets in addition to Bcl-x_L. Poor specificity should not necessarily be considered as detrimental, however, since it is anticipated that inhibiting several anti-apoptotic proteins should potentiate a small-molecule's anti-tumour activity.[43]

In conclusion, we have investigated the significance of the backbone identity of a series of oligoamide-foldamer-based α-helix mimetics in the context of disruption of the Bak–Bcl-x_L complex through effective mimicry of the Bak BH3 α-helix. The present results indicate that oligoamides of greater benzene-to-pyridine ratios are more potent Bcl-x_L inhibitors. This appears to be a consequence of both a greater capacity to assume more favourable binding conformations, through a reduction of intramolecular bifurcated hydrogen bonding, as well as presenting increased hydrophobic surfaces that better complement the Bcl-x_L hydrophobic crevice. Our compounds were also effective at inhibiting the proliferation of cancer cells that overexpress Bcl-x_L. Other proteins of the Bcl-2 family, specifically Bcl-2 and Mcl-1, are also up-regulated in various cancers.[19,20] ABT-737 is an especially potent Bcl-2/Bcl-x_L inhibitor but demonstrates

limited activity against Mcl-1.[25,44] It is expected that small-molecule BH3 mimetics that bind only Bcl-2 and Bcl-x_L but not Mcl-1 might lead to resistant tumors through high expression levels of Mcl-1, and this has, indeed, been observed with ABT-737.[44] Therefore, future work is aimed at developing pan-Bcl-2 inhibitors using a structure-based design strategy that includes modeling of protein–BH3 α-helix mimetic interactions. Our results will be reported in due course.

Acknowledgements

We are grateful to Prof. Jean-Marie Hardwick (Johns Hopkins University) for the generous gift of Bcl-x_L. We thank the University of Maryland School of Pharmacy (SF), the University of Maryland Computer-Aided Drug Design Center (ADM), the American Association of Colleges of Pharmacy (AACP) New Pharmacy Faculty Research Award (SF) and NSF CHE-0823198 (ADM) for financial support of this work. Additionally, these studies were supported by the Center for Biomolecular Therapeutics, the University of Maryland School of Medicine and the Institute for Bioscience and Biotechnology Research.

Notes and references

1 T. A. Edwards and A. J. Wilson, *Amino Acids*, 2011, **41**, 743.
2 C. G. Cummings and A. D. Hamilton, *Curr. Opin. Chem. Biol.*, 2010, **14**, 341.
3 J. M. Davis, L. K. Tsou and A. D. Hamilton, *Chem. Soc. Rev.*, 2007, **36**, 326.
4 S. Fletcher and A. D. Hamilton, *Curr. Opin. Chem. Biol.*, 2005, **9**, 632.
5 B. P. Orner, J. T. Ernst and A. D. Hamilton, *J. Am. Chem. Soc.*, 2001, **123**, 5382.
6 O. Kutzki, H. S. Park, J. T. Ernst, B. P. Orner, H. Yin and A. D. Hamilton, *J. Am. Chem. Soc.*, 2002, **124**, 11838.
7 H. Yin, G. I. Lee, K. A. Sedey, O. Kutzki, H. S. Park, B. P. Orner, J. T. Ernst, H. G. Wang, S. M. Sebti and A. D. Hamilton, *J. Am. Chem. Soc.*, 2005, **127**, 10191.
8 H. Yin, G. I. Lee, H. S. Park, G. A. Payne, J. M. Rodriguez, S. M. Sebti and A. D. Hamilton, *Angew. Chem., Int. Ed.*, 2005, **44**, 2704.
9 J. T. Ernst, J. Becerril, H. S. Park, H. Yin and A. D. Hamilton, *Angew. Chem., Int. Ed.*, 2003, **42**, 535.
10 F. Campbell, J. P. Plante, T. A. Edwards, S. L. Warriner and A. J. Wilson, *Org. Biomol. Chem.*, 2010, **8**, 2344.
11 C. G. Cummings, N. T. Ross, W. P. Katt and A. D. Hamilton, *Org. Lett.*, 2009, **11**, 25.
12 S. Marimganti, M. N. Cheemala and J. M. Ahn, *Org. Lett.*, 2009, **11**, 4418.
13 P. Maity and B. Konig, *Org. Lett.*, 2008, **10**, 1473.
14 S. M. Biros, L. Moisan, E. Mann, A. Carella, D. Zhai, J. C. Reed and J. Rebek Jr, *Bioorg. Med. Chem. Lett.*, 2007, **17**, 4641.
15 A. Volonterio, L. Moisan and J. Rebek Jr, *Org. Lett.*, 2007, **9**, 3733.
16 N. N. Danial and S. J. Korsmeyer, *Cell*, 2004, **116**, 205.
17 K. W. Yip and J. C. Reed, *Oncogene*, 2008, **27**, 6398.
18 X. Cao, C. Rodarte, L. Zhang, C. D. Morgan, J. Littlejohn and W. R. Smythe, *Cancer Biol. Ther.*, 2007, **6**, 246.
19 H. Zhang, S. Guttikonda, L. Roberts, T. Uziel, D. Semizarov, S. W. Elmore, J. D. Leverson and L. T. Lam, *Oncogene*, 2011, **30**, 1963.
20 H. Zhang, Y. Li, Q. Huang, X. Ren, H. Hu, H. Sheng and M. Lai, *Cell Death Differ.*, 2011, **18**, 1702.
21 J. M. Adams and S. Cory, *Oncogene*, 2007, **26**, 1324.
22 J. M. Adams and S. Cory, *Science*, 1998, **281**, 1322.
23 M. Sattler, H. Liang, D. Nettesheim, R. P. Meadows, J. E. Harlan, M. Eberstadt, H. S. Yoon, S. B. Shuker, B. S. Chang, A. J. Minn, C. B. Thompson and S. W. Fesik, *Science*, 1997, **275**, 983.
24 M. Vogler, D. Dinsdale, M. J. Dyer and G. M. Cohen, *Cell Death Differ.*, 2009, **16**, 360.
25 D. Zhai, C. Jin, A. C. Satterthwait and J. C. Reed, *Cell Death Differ.*, 2006, **13**, 1419.
26 T. Oltersdorf, S. W. Elmore, A. R. Shoemaker, R. C. Armstrong, D. J. Augeri, B. A. Belli, M. Bruncko, T. L. Deckwerth, J. Dinges, P. J. Hajduk, M. K. Joseph, S. Kitada, S. J. Korsmeyer, A. R. Kunzer, A. Letai, C. Li, M. J. Mitten, D. G. Nettesheim, S. Ng, P. M. O' Nimmer, J. M. Connor, A. Oleksijew, A. M. Petros, J. C. Reed, W. Shen, S. K. Tahir, C. B. Thompson, K. J. Tomaselli, B. Wang, M. D. Wendt, H. Zhang, S. W. Fesik and S. H. Rosenberg, *Nature*, 2005, **435**, 677.
27 B. D. Zeitlin, E. Joo, Z. Dong, K. Warner, G. Wang, Z. Nikolovska-Coleska, S. Wang and J. E. Nor, *Cancer Res.*, 2006, **66**, 8698.
28 G. Tang, Z. Nikolovska-Coleska, S. Qiu, C. Y. Yang, J. Guo and S. Wang, *J. Med. Chem.*, 2008, **51**, 717.
29 J. Wei, S. Kitada, M. F. Rega, A. Emdadi, H. Yuan, J. Cellitti, J. L. Stebbins, D. Zhai, J. Sun, L. Yang, R. Dahl, Z. Zhang, B. Wu, S. Wang, T. A. Reed, H. G. Wang, N. Lawrence, S. Sebti, J. C. Reed and M. Pellecchia, *Mol. Cancer Ther.*, 2009, **8**, 904.
30 I. Saraogi, C. D. Incarvito and A. D. Hamilton, *Angew. Chem., Int. Ed.*, 2008, **47**, 9691.
31 J. Plante, F. Campbell, B. Malkova, C. Kilner, S. L. Warriner and A. J. Wilson, *Org. Biomol. Chem.*, 2008, **6**, 138.
32 B. R. Brooks, C. L. Brooks 3rd, A. D. Mackerell Jr., L. Nilsson, R. J. Petrella, B. Roux, Y. Won, G. Archontis, C. Bartels, S. Boresch, A. Caflisch, L. Caves, Q. Cui, A. R. Dinner, M. Feig, S. Fischer, J. Gao, M. Hodoscek, W. Im, K. Kuczera, T. Lazaridis, J. Ma, V. Ovchinnikov, E. Paci, R. W. Pastor, C. B. Post, J. Z. Pu, M. Schaefer, B. Tidor, R. M. Venable, H. L. Woodcock, X. Wu, W. Yang, D. M. York and M. Karplus, *J. Comput. Chem.*, 2009, **30**, 1545.
33 K. Vanommeslaeghe, E. Hatcher, C. Acharya, S. Kundu, S. Zhong, J. Shim, E. Darian, O. Guvench, P. Lopes, I. Vorobyov and A. D. Mackerell Jr, *J. Comput. Chem.*, 2010, **31**, 671.
34 D. L. Warren, *PyMOL*, Delano Scientific, San Carlos, CA, 2002.
35 *ChemBioDraw*, Cambridgesoft, Cambridge, MA, 2009.
36 G. C. Hopkins, J. P. Jonak, H. J. Minnemeyer and H. Tieckelmann, *J. Org. Chem.*, 1967, **32**, 4040.
37 J. L. Yap, K. Hom and S. Fletcher, *Tetrahedron Lett.*, 2011, **52**, 4172.
38 H. Zhang, P. Nimmer, S. H. Rosenberg, S. C. Ng and M. Joseph, *Anal. Biochem.*, 2002, **307**, 70.
39 Y. Cheng and W. H. Prusoff, *Biochem. Pharmacol.*, 1973, **22**, 3099.
40 S. Wu, H. Zhu, J. Gu, L. Zhang, F. Teraishi, J. J. Davis, D. A. Jacob and B. Fang, *Cancer Res.*, 2004, **64**, 1110.
41 X. Cao, J. Littlejohn, C. Rodarte, L. Zhang, B. Martino, P. Rascoe, K. Hamid, D. Jupiter and W. R. Smythe, *Am. J. Pathol.*, 2009, **175**, 2207.
42 M. D. Cummings, C. Schubert, D. J. Parks, R. R. Calvo, L. V. LaFrance, J. Lattanze, K. L. Milkiewicz and T. Lu, *Chem. Biol. Drug Des.*, 2006, **67**, 201.
43 K. Kojima, M. Konopleva, I. J. Samudio, W. D. Schober, W. G. Bornmann and M. Andreeff, *Cell Cycle*, 2006, **5**, 2778.
44 M. F. van Delft, A. H. Wei, K. D. Mason, C. J. Vandenberg, L. Chen, P. E. Czabotar, S. N. Willis, C. L. Scott, C. L. Day, S. Cory, J. M. Adams, A. W. Roberts and D. C. Huang, *Cancer Cell*, 2006, **10**, 389.